Changes in Fibroblast Mechanostat Set Point and Mechanosensitivity: An Adaptive Response to Mechanical Stress in Floppy Eyelid Syndrome

Daniel G. Ezra,[1,2,3] *James S. Ellis,*[1,4] *Michèle Beaconsfield,*[2] *Richard Collin,*[2] *and Maryse Bailly*[3]

Purpose. Floppy eyelid syndrome (FES) is an acquired hyperelasticity disorder affecting the upper eyelid. The tarsal plate becomes hyperelastic with a loss of intrinsic rigidity. As a result, the eyelid is subjected to cyclic mechanical stress. This condition was used as a model to investigate changes in dynamic fibroblast contractility in the context of chronic cyclic mechanical stress.

Methods. Contractile efficiency was investigated in a free-floating, three-dimensional collagen matrix model. Intrinsic cellular force measurements and responses to changes in gel tension were explored using a tensioning culture force monitor (t-CFM). Gene expression differences between cell lines exhibiting differences in contractile phenotype were explored with a genome level microarray platform and RT-PCR.

Results. FES tarsal plate fibroblasts (TFs) showed an increased contractile efficiency compared with the control, and t-CFM measurements confirmed a higher intrinsic cellular force at plateau levels. Cyclic stretch/relaxation experiments determined that TFs in FES maintained a functional tensional homeostasis response but with an altered sensitivity, operating around a higher mechanostat set point. Gene expression array and RT-PCR analysis identified V-CAM1 and PPP1R3C as being upregulated in FES TFs.

Conclusions. These changes may represent an adaptive response that allows tensional homeostasis to be maintained at the high levels of tissue stress experienced in FES. Gene expression studies point to a role for V-CAM1 and PPP1R3C in mediating changes in the dynamic range of mechanosensitivity of TFs. This work identifies FES as a useful model for the study of adaptive physiological responses to mechanical stress. (*Invest Ophthalmol Vis Sci.* 2010;51:3853–3863) DOI:10.1167/iovs.09-4724

Cells exposed to external mechanical loading change their contractile behavior to maintain optimal intrinsic tension. This process is described as tensional homeostasis,[1] and it allows cells to maintain an appropriate level of cytoskeletal tension against a background of changing tissue stress.[2] The tensional homeostasis response predicts that cells will reduce their contractility in high-stress environments and conversely increase their contractility in low-stress environments to maintain a balance between external and internal tension.

Forces acting on the extracellular matrix (ECM) are thought to be sensed by the cell through cell surface/ECM connections. Little is known about the mechanisms involved in maintaining tensional homeostasis, but mechanotransduction is believed to be mediated by mechanosensitive cell membrane integrin complexes at sites of attachment of the cell to the surrounding matrix. Subsequent changes in cell contraction are thought to be a result of actin cytoskeleton reorganization which may involve the formation of new stress fibers at high tissue stress levels.[3–6]

In fibroblasts, changes in cell morphology have been observed in response to changes in the mechanical environment of the cell.[6] In addition to inducing morphologic changes, mechanical stimuli can elicit functional changes. Fibroblasts embedded in a three-dimensional collagen matrix respond to external forces by modulating their contractility. Increased external loading is met by a diminution of cellular contraction, and decreased external loading is met by a corresponding increase in contractility.[2] These observed patterns of behavior were found to be consistent across a range of different matrix stiffnesses, suggesting that they are an intrinsic cell property and not simply dependent on the mechanical status of the matrix.

This homeostasis system operates between tolerated bands of tissue tension within which the balance between internal cytoskeletal tension and external tension can be maintained, a concept first described by Frost[7] as the mechanostat set point. However, several studies suggest that the threshold range of mechanical sensitivity for a given cell type may vary[2,8] as an adaptation response to changes in the environment.[9,10] Using MMP-13 production as a surrogate marker for variation in cell mechanoresponsiveness, Arnoczky et al.[9] have recently demonstrated that if homeostatic tissue tension is lost for prolonged periods, tendon cells reset their mechanostat levels so that a greater level of mechanical stress is needed to generate a response. As the field of tissue engineering and repair is fast expanding, unraveling the mechanisms underlying tensional homeostasis and adaptive response to mechanical stress is an

From the [1]National Institute of Health Research (NIHR) Biomedical Research Centre for Ophthalmology, Moorfields Eye Hospital and UCL Institute of Ophthalmology, and the [2]Adnexal Department, Moorfields Eye Hospital, London, United Kingdom; and the Departments of [3]Cell Biology and [4]Ocular Biology and Therapeutics, UCL Institute of Ophthalmology, London, United Kingdom.

Supported by the special trustees of Moorfields Eye Hospital (DGE); Medical Research Council (MRC) Grant G0500927 (MB); and partial support from the Department of Health through an award made by the NIHR to Moorfields Eye Hospital NHS Foundation Trust and UCL Institute of Ophthalmology for a Specialist Biomedical Research Centre for Ophthalmology. Laboratories and imaging facilities were supported by the Wellcome Trust and the MRC. The views expressed in this publication are those of the authors and not necessarily those of the Department of Health. This manuscript forms part of a doctoral thesis submitted to Cambridge University (DGE).

Submitted for publication October 2, 2009; revised February 4, 2010; accepted February 5, 2010.

Disclosure: **D.G. Ezra**, None; **J.S. Ellis**, None; **M. Beaconsfield**, None; **R. Collin**, None; **M. Bailly**, None

Corresponding author: Daniel G. Ezra, NIHR Biomedical Research Centre for Ophthalmology, Moorfields Eye Hospital and UCL Institute of Ophthalmology, London EC1V 2PD, UK; d.ezra@ucl.ac.uk.

essential step toward the reconstruction of fully functional tissues.

Floppy eyelid syndrome (FES) is an acquired hyperelasticity disorder affecting the upper eyelid. The upper eyelid is a composite structure consisting of skin, orbicularis oculi muscle fibers, tarsal plate, and conjunctiva in an anterior-to-posterior sequence (see Fig. 1). The tarsal plate consists of dense collagenous fibrous tissue running along the width of the upper eyelid. It is the stiffest component that acts to maintain the integrity of the upper eyelid and prevent distortion.[11] In FES, the tarsal plate ECM undergoes dramatic biomechanical changes, becoming pliant and hyperelastic, allowing the upper lid to become everted with ease and exposing the ocular surface, causing papillary conjunctivitis and exposure keratopathy.[12] Although this condition most often results in severe discomfort, serious complications including corneal vascularization and scarring,[13,14] ulcerative microbial keratitis,[15,16] and corneal perforations[17,18] have been widely reported. The etiology of the disease is unknown, although a decrease in mature elastic fiber abundance in the tarsal plate[16,19] and an associated upregulation of elastase MMP activity have been identified.[13] Treatment has been limited to surgically restoring tension to the tarsal plate by resecting and tightening the upper eyelid.[20]

There is a significant association between the laterality of the condition and sleeping side,[21] as exposure of the ocular surface occurs at night by way of the upper lid's being distorted by interaction with the pillow.[12] The result is that the upper lid is exposed to recurrent pathologic cyclic loading and eversion at night, thus providing a model for how chronic cyclic tissue stress could affect cell mechanostat levels. As FES involves both changes in the biomechanical properties of the ECM and also pathologic cyclic tissue loading, we hypothesized that cells in the affected tissue may present a dysregulated tensional homeostasis response. The purposes of this study were to investigate how the intrinsic cellular force generated by fibroblasts is altered in the context of FES, as well as the nature of any change in tensional homeostasis response and associated changes in gene expression.

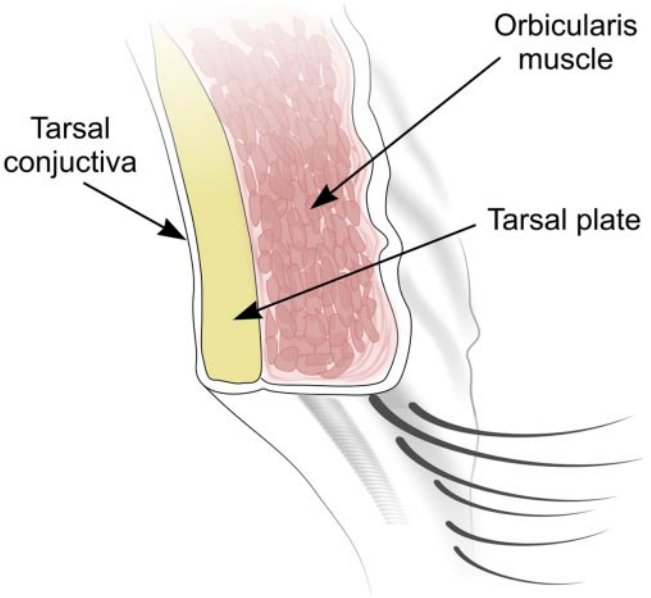

FIGURE 1. Cross section of the upper eyelid demonstrating the basic anatomy of its major structural components.

MATERIALS AND METHODS

Tissue Harvesting and Cell Culture

Full-thickness upper lid tissue was harvested from patients who were undergoing upper lid tightening for the treatment of FES. Full regional ethics committee approval was granted in accordance with the Declaration of Helsinki. Three different upper lid tissues providing the greatest contribution to the mechanical integrity of the upper eyelid were studied: the orbicularis oculi muscle, the tarsal plate, and conjunctiva (see Fig. 1 for a schematic representation of the anatomic layers of the upper eyelid). Five full-thickness samples were obtained. A corresponding number of healthy control tissues were collected from tumor reconstruction (after tumor excision), blepharoplasty, and ptosis surgery. No patients received radiotherapy. Primary cell cultures were derived from these different tissue types. Tarsal tissues were cut into small pieces and subjected to collagenase digestion (5% collagenase diluted 1:10 in Dulbecco's phosphate-buffered saline; DPBS, cat. no. 14040; Invitrogen-Gibco, Paisley, UK) for 10 minutes before plating. The conjunctiva and orbicularis tissues were cut into small pieces. The tissue fragments were plated onto T25 culture flasks (Nunc, Rochester, NY) and maintained in medium consisting of DMEM (Dulbecco's modified Eagle's medium) with 4500 mg/mL glucose, L-glutamine, and pyruvate (cat. no. 41966; Invitrogen-Gibco), with 10% fetal bovine serum (FBS cat. no. F9665; Sigma-Aldrich, Poole, UK), 100 U/mL of penicillin, 100 U/mL of streptomycin, and 2 nM L-glutamine (cat. no. 25030; Invitrogen-Gibco). The cells were maintained in complete medium in tissue culture incubators with 5% CO_2 and at 95% humidity at 37°C. The cells that had reached confluence were passaged and split at a ratio of 1:4.

Collagen-Contraction Assay

Free-floating, fibroblast-seeded, three-dimensional collagen matrices were prepared according to a previously described method.[22] In brief, a collagen gel solution was prepared with 830 μL of rat tail type I collagen in acetic acid (2.1 mg/mL in 0.6% acetic acid, cat. no. 60-30-810; First Link, Birmingham, UK) to which 160 μL of concentrated medium (made up from 3.5 mL 10× DMEM [Sigma-Aldrich]; 150 μL L-glutamine, cat. no. 25030 [Invitrogen-Gibco]; and 900 μL sodium bicarbonate 7.5% S8761 [Sigma-Aldrich]) were added. The collagen solution was then rapidly adjusted to pH 7.0 with NAOH, to induce collagen polymerization. A variety of different cell concentrations (at passages 3–4) were used to determine which concentration would allow the sensitivity of the test to differentiate best between diseased and control cell lines. A cell suspension containing the desired number of cells (1×10^5) was centrifuged at 1400 rpm for 4 minutes. Supernatant was aspirated and the cell pellet resuspended in serum. The cell suspension was then added to the collagen solution and gently mixed. The cell-seeded collagen suspensions were then cast into the shape of 150-μL buttons of 14 mm diameter, using the central well of a 35-mm glass-bottomed culture dish (MatTek Corp., Ashland, MI) as a mold. The buttons were then placed in a tissue culture incubator. After 30 minutes of polymerization at 37°C, the buttons were manually detached from the central well by scoring the circumference of the well with a needle. The nascent gels were then floated in medium and placed in the incubator. Whole matrix contraction was measured by using digital photography immediately after the release of the polymerized matrix (t_0) and then every 24 hours for 7 days (t_x). Images were imported onto ImageJ 1.40g software (developed by Wayne Rasband, National Institutes of Health, Bethesda, MD; available at http://rsb.info.nih.gov/ij/index.html). Gel surface area was normalized to the area calculated at t_0 by the following formula: $A(t_x) = 100 - (100r_{tx}^2/r_{t0}^2)$ where A is the percentage of initial gel surface area, and r is the radius. Matrix-contraction assays were conducted in all cell lines in triplicate. A set of acellular gels was cast for the control experiments. Cell viability was assessed in gels containing conjunctival and TFs by using trypan blue staining at days 1 and 6.

Force Measurements and External Tension Modification

We used our custom-built tensioning-culture force monitor (t-CFM)[22–24] to measure the minute forces exerted by fibroblasts contracting within an in vitro collagen matrix with a force transducer that accurately converts mechanical deflection of a sensor into a digital signal after calibration with weights. Force measurements were made in dynes (1 dyne = 10^{-5} Newtons). The force value at equilibrium, or intrinsic cellular force,[22] is a reflection of the mechanostat level for individual cells.[2]

For the t-CFM experiments, larger cell-seeded collagen gels were cast (composed of 2145 μL of type I collagen stock, and 414 μL of concentrated medium made of 1750 μL of concentrated DMEM, 450 μL of sodium bicarbonate 7.5%, and 175 μL of L-glutamate). Cells (1×10^6 at passages 3–4) were resuspended in 290 μL of FBS and then added to the collagen solution. The collagen solution was quickly cast into a custom-built mold measuring 25 × 15 mm. Flotation bars made from a synthetic solid porous polymeric material with hydrophilic properties that can be cut into strips or blocks (Vyon; Porvair, Hampshire, UK) were set at the extreme ends of the gel mold. The porous architecture of the bars allowed them to become integrated into the gel complex. Metal fixation hooks were fashioned from wire to allow the flotation bars to fix to the t-CFM fixation points.

After the gel had set, it was cut from the mold and lifted into a 35-mm culture dish. Leibowitz's L-15 medium (cat. no. 21083; Invitrogen-Gibco) with 10% FBS was added until the gel was submerged. One to 2 mL of heavy mineral oil was then added to cover the aqueous culture medium to prevent its evaporation. Force measurements were recorded every 10 seconds for 12 hours.

The t-CFM was also used to investigate the contractile responses of the resident cells in the collagen matrix to external loading or relaxation. A microstepping motor and control unit (Micromech Systems, Ltd., Braintree, UK) in conjunction with a precision-ground lead screw is incorporated in the design, allowing movement of the stage to an accuracy of 1×10^{-8} m^2.

Fibroblast populated gels were allowed to contract undisturbed for 8 hours to allow enough time for the cells to generate appropriate adhesions with the surrounding collagen matrix.[2] The cells were then subjected to cyclic loading and unloading. Fibroblast-populated gels were first subjected to a loading phase of approximately 10 dynes above baseline for 30 minutes and then relaxed to approximately 10 dynes below baseline. This cycle was repeated five times. The cyclic loading frequency was based on previous work by Brown et al.[2] and optimized to allow a maximum response for the TFs. Three FES TF cell lines and three control TF cell lines were chosen, and all experiments were performed in triplicate. During the stress–relaxation experiments, a change in gel tension of approximately 5 to 10 dynes above and below the plateau level was applied. Each relaxation and contraction experiment consisted of five contraction phases and five relaxation phases. For each experiment, the means of the five gradient responses for contraction and the five gradient responses for relaxation of the gels (the measurement of the gradient response is illustrated in Fig. 4B), were recorded. In addition, the average force value at tensional homeostasis (baseline plateau phase, illustrated in Figs. 3, 4) was taken as additional data, because baseline levels of tension delivered a rate of change of intrinsic cellular force of 0 (as no relaxation or contraction effect is observed with the cell at tensional homeostasis). The mean rate of change of contraction was then plotted against the mean force applied by the t-CFM, which generated that response. Triplicate experiments were performed for three FES TF cell lines and three control TF cell lines, providing a total of 27 data points for FES and control cell lines.

Finally, control experiments were performed with collagen gels cast without any embedded cells to exclude any changes in tension arising from the viscoelastic properties of the gel itself. As a control for FES cell lines, the acellular gel was pretensioned to match the mean baseline of the three FES TF cell lines used. For control TF cell lines, the gel was pretensioned at the mean baseline for the three control cells.

Immunofluorescence

Simultaneous filamentous actin (F-actin) and α-smooth muscle actin (α-SMA) immunofluorescent labeling was performed in accordance to the method described by Bailly et al.[25] Cells at passages 3 to 4 were plated on coverslips and the next day were fixed with 3.7% formaldehyde for 5 minutes. The cells were then permeabilized with 0.5% Triton X-100 (T92845; Sigma-Aldrich) in cytobuffer[25] for 20 minutes, followed by a rinse in 0.1 M glycine in cytobuffer for 10 minutes. Nonspecific staining was blocked, and F-actin was simultaneously labeled by adding TBS/1% bovine serum albumin (BSA) and 1% FBS together with 1:300 dilution of FITC-labeled fluorescent phalloidin (Alexa Fluor 488 phalloidin, A-12379; Invitrogen-Molecular Probes; Eugene, OR) in a humidified chamber for 30 minutes. The phalloidin and block were aspirated, and primary antibody to α-SMA was added (A5228; Sigma-Aldrich) at a dilution of 1:100 and incubated in a humidified chamber for 1 hour. The samples were then rinsed in TBS five times for 5 minutes and incubated with a secondary antibody (TRITC anti-mouse; Jackson ImmunoResearch, West Grove, PA) in a dilution of 1:80 for another hour. Finally, the specimens were washed five times for 5 minutes with TBS and mounted on slides.

A similar method was used for the staining of cells that had been embedded in collagen gels, but using higher concentrations of FITC-phalloidin (1:60), anti α-SMA (1:75), and TRITC anti-mouse secondary antibody (1:40). The incubation period for the primary antibody was extended to overnight in 4°C, to allow for adequate penetration of the gel, and the rinse cycles were lengthened to 20 minutes per wash. The gels were mounted in the central well of a culture (MatTek) dish.

Confocal laser microscopy was performed on these samples (Axiovert S100 TV; Carl Zeiss Meditec, Inc., Welwyn Garden City, UK, or Radiance 2000; Bio-Rad, Hemel Hempstead, UK), with appropriate light wavelengths and a long-working-distance ×60 air objective (63×/0.75 plan Neofluar with correction collar; Carl Zeiss Meditec, Inc.) for gels mounted in culture dishes (MatTek) and a standard ×60 oil-immersion objective (63X/1.4 Plan Apochromat; Carl Zeiss Meditec, Inc.) for coverslips mounted on slides. The proportion of α-SMA-expressing cells was determined by cell counting in five random fields for each of five control and five test gels, with a total of 103 and 94 cells counted for each set, respectively.

mRNA Expression Profiling

RNA extraction from cultured fibroblasts of both FES tarsal tissue and control tarsal tissue was performed at passage 3. RNA extraction was performed from five TF FES cell lines and five TF control cell lines. Confluent cells from a T25 flask were trypsinized and spun down. RNA isolation was performed in accordance with the manufacturer's protocols (RNEasy kit; Qiagen, Hilden, Germany). Quantity and purity of RNA Total RNA was quantified using the spectrophotometer (NanoDrop; Thermo Scientific, Wilmington, DE). Excess RNA was then stored at −80°C.

mRNA from three TF FES and three TF control cell lines was analyzed with a cDNA microarray platform (GeneChip Human Gene 1.0ST; Affymetrix, Santa Clara, CA). All microarray analysis was performed according to the manufacturer's protocol by UCL Genomics at the Institute of Child Health microarray laboratory, Institute of Child Health (London, UK). Briefly, RNA was again assessed for quality, integrity, quantity, and purity, using both the spectrophotometer (NanoDrop) and a bioanalyzer (model 2100; Agilent, Santa Clara, CA). Total RNA was reverse transcribed to cDNA and labeled (GeneChip; WT Sense Target Labeling kit and control reagents; Affymetrix). Labeled cDNA was hybridized to the array chip according to standard Affymetrix protocols. The chip was then washed in a wash station (Affymetrix) by using the standard wash protocols, and then scanned (GeneChip 3000 7G Scanner; Affymetrix) and data collected as .dat files before conversion to .cel files for analysis.

Gene array .cel files were analyzed (Genespring GX version 10.01 2100; Agilent). Briefly, gene level expression values were generated with the robust multiarray average (RMA).[26] An expression level filter was then applied to exclude the genes expressed at levels below detection limits in both groups (20% intensity in more that four of six samples). A total of 13,500 genes passed this filtering process, and a nonparametric Welch's *t*-test was then used to test for differences in individual gene expression.

Candidate genes with significant differences ($P < 0.05$) in expression were further investigated with semiquantitative RT-PCR. RNA was reverse transcribed to cDNA (First-Strand cDNA synthesis kit, cat. no. 4379012001; Roche Diagnostics, Mannheim, Germany) and incubated using a PCR cycler (Mastercycler Gradient; Eppendorf, AG, Hamburg, Germany) according to the manufacturer's instructions. Either 1 μL (*GAPDH*) or 1.5 μL (other genes) of cDNA was further used in the PCR step with master mix (Megamix Blue; Helena Biosciences, Gateshead, UK), according to the manufacturer's protocol. Sequences of forward and reverse primers are provided in Table 1. cDNA was then polymerized in the same PCR cycler (Mastercycler; Eppendorf, AG), with an initial denaturation step of 94°C for 2 minutes, the PCR cycle was then programmed to denature the DNA strands at 94°C for 30 seconds, followed by an annealing temperature of either 55°C (*GAPDH*) or 60°C for other primers. DNA was then polymerized at 72°C for 1 minute. The number of cycles varied between 29 and 33 cycles (Table 1). The final polymerization step at 72°C was programmed for 7 minutes. At the end of this cycle, the reaction mix was cooled to 4°C.

Agarose gels were made by heating 1% agarose in TAE buffer for 2 minutes. Fourteen μL red nucleic acid stain (Gel Red; Biotium, Hayward, CA) was then added to the gel, which was cast into a gel mold with the desired comb. The gel was allowed to set for at least 30 minutes. The sample (12 μL) was loaded into the gel after centrifugation and mixing with the pipette. The gel was then run in an electrophoresis tank (Bio-Rad) for 60 minutes at 140 V. Bands were visualized using the G-box gel imaging system (Syngene, Bangalore, India). The intensity was adjusted to the point where visualization of each band was possible with minimal saturation. Typically, each gel was exposed for between 0.04 and 0.4 seconds, depending on the gene expression. After capture, each image was saved in .tif format and imported into ImageJ 1.40g software. Band optical density was then quantified by using the in-built gel-analysis software. Gene expression was quantified by normalizing each gene to *GAPDH* expression. RT-PCR analysis of the *GAPDH* gene was repeated several times to ensure accuracy. A two-way Mann-Whitney U test (95% CI) was used to determine statistical significance. $P < 0.05$ was considered significant.

Results

Altered Matrix Contraction Efficiency in FES Tarsal Fibroblasts

No difference in matrix contraction efficiency between FES and the control was demonstrated for conjunctival or orbicularis fibroblasts (Figs. 2A, 2B). The cells broadly contracted the matrix by around 50% within the first day, although there was more variability in the matrix contraction of orbicularis fibroblasts by the first day, varying from 40% to 55%. The contraction continued at a slower rate, thereafter reaching a plateau at days 4 to 5.

Control TFs surprisingly showed a significantly lower level of matrix contraction, both in terms of early contraction rate and final plateau phase (Fig 2C). Control TF-seeded matrices contracted by 10% to 30% by day 1 compared with 40% to 65% for FES TFs. The plateau achieved by these different cell lines also differed significantly ($P = 0.0002$, paired *t*-test) with control TF-seeded matrices achieving a contraction of only 50% to 65% compared with a contraction of around 65% to 90% for FES TFs. No difference in cell viability counts between the control and FES tarsal cell lines at day 1 (99.2%, SD 0.51% and 98.6%, SD 0.53%, viability respectively; $P = 0.2$) and day 6 (96.8%, SD 0.53% and 96.3%, SD 0.39%, viability respectively; $P = 0.26$) were identified.

Altered Contractile Force in FES Tarsal Fibroblasts

Force-generation graphs were produced for each of the five FES and five control tarsal cell lines. Figure 3 illustrates the resulting individual force generation curves, demonstrating significant differences between the control and FES cell lines. First, the plateau levels reached by the different TF groups are significantly different ($P < 0.0001$, paired *t*-test). The FES TFs produce a much higher plateau of force generation of between 33 and 53 dynes/million cells. The control TFs produce a significantly lower plateau of force generation of between 5 and 35 dynes/million cells (mean, 44 dynes/million cells), with most of the cell lines clustering at a plateau region of 5 to 12 dynes/million cells (mean, 16 dynes/million cells). Second, the time taken to achieve the plateau phase was longer for the FES TFs, which reached a plateau at between 4 and 8 hours (average, 7 hours), whereas the control TFs achieved a plateau at between 2 and 5 hours (average, 5 hours; Fig. 3). Finally, the early contraction rate (slope of the curve at growing phase) was significantly higher for the FES cells than for the control (Fig. 3B).

Table 1. Description of Primers Used for RT-PCR

Gene	Primer Sequence	Size (bp)	Annealing Temp. (°C)	Cycles (*n*)
VCAM1 F	AGTCAGGAATTTCTGGAGGATGC	229	60	31
VCAM1 R	GCAGCTTTGTGGATGGATTCAC			
VERSICAN F	TCAACATCTCATGTTCCTCCC	336	60	32
VERSICAN R	TTCTTCACTGTGGGTATAGGTCTA			
EFEMP1 F	TGCCATCAGACATCTTCCAG	292	60	32
EFEMP1 R	TGCCTGTGGTTGACTCTTAGAA			
PPP1R3C F	TTTTAACATGTGTGATGTGCCA	151	60	31
PPP1R3C R	ATTCTTAAAGTGAGAAGCTCATCAA			
CCBE1 F	CCTGGTTCTTTCGACTTCCTGCTA	181	60	32
CCBE1 R	TTCTTGGATGGTCATCTCCAGAGCC			
PRSS12 F	GAGAGGTCCTTGGCTGACTG	569	60	32
PRSS12 R	GAGAGGTCCTTGGCTGACTG			
GAPDH F	CCACCCATGGCAAATTCCATGGCA	598	55	30
GAPDH R	TCTAGACGGCAGGTCAGGTCCACC			

F, forward; R, reverse.

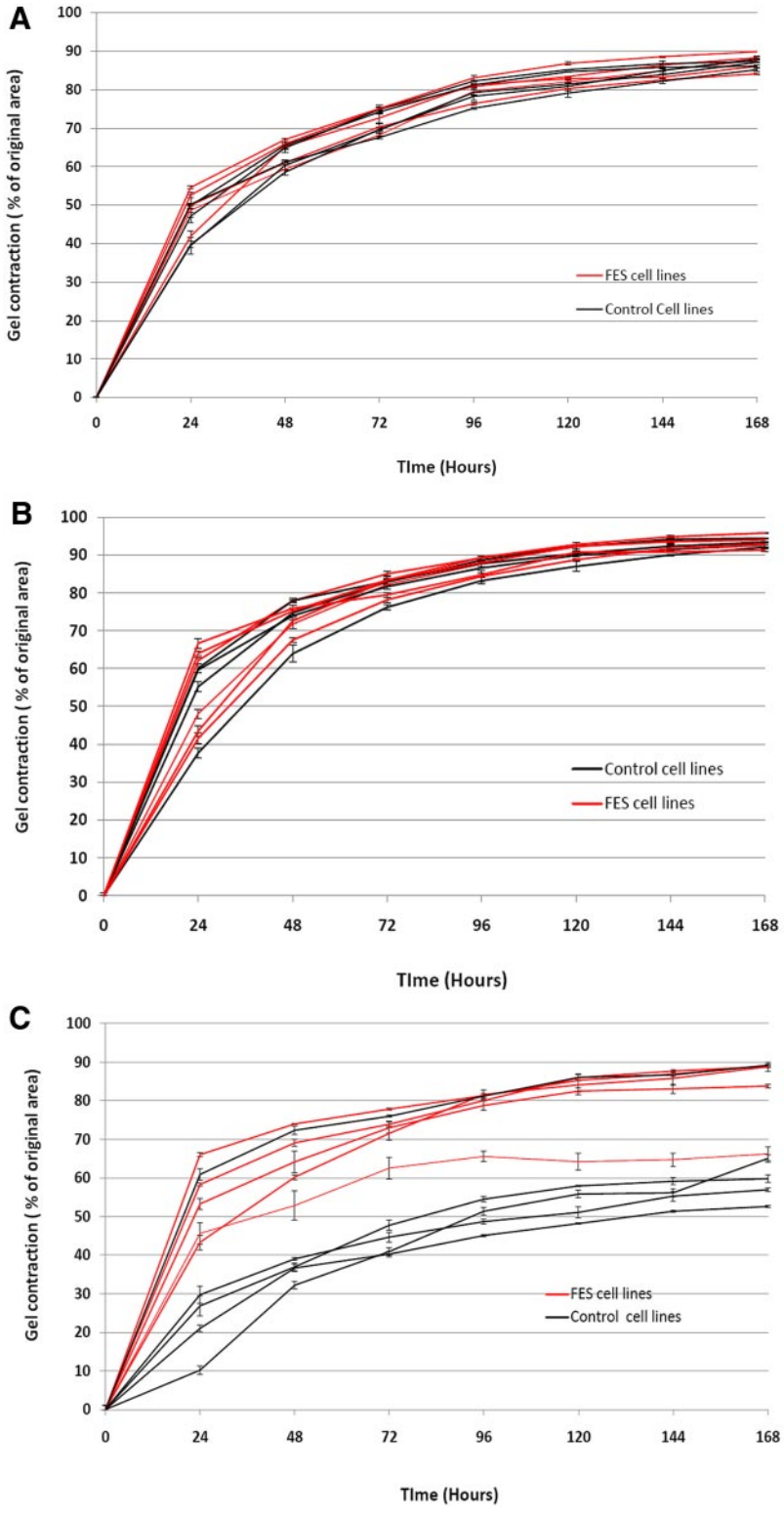

FIGURE 2. Cell-mediated collagen gel contraction was affected in FES tarsal plate fibroblasts. Fibroblast cell lines derived from control and FES tissue were seeded in collagen gels and matrix contraction in presence of 10% FBS was recorded over 7 days. In each graph, five FES cell lines and five control cell lines are represented, with mean ± SEM for a minimum of three experiments, each in triplicate. (**A**) Contraction profiles of conjunctival fibroblasts. (**B**) Contraction profiles of orbicularis fibroblasts. (**C**) Contraction profiles of tarsal plate fibroblasts. Significant differences were observed at plateau level by TFs ($P < 0.02$, *t*-test) only with no significant differences evident with either conjunctival or orbicularis fibroblasts.

Tensional Homeostasis and the Mechanostat Set Point in FES Tarsal Fibroblasts

To determine whether FES TFs present altered mechanosensitivity, the cells in the gels were submitted to multiple loading and relaxation cycles, and the response of the cells was monitored with the tensioning culture force monitor (t-CFM; Fig. 4A). As predicted from the expected tensional homeostasis levels, loading steps (gel stretch) on gels populated with control fibroblasts resulted in an immediate reduction in the endogenous force generated by the cells. Conversely, relaxation below the normal force value at plateau resulted in an immediate increase in endogenous force as the cells strive to maintain their preferred level of tension (force at plateau level).

Although the FES cells presented much higher levels of force at tensional homeostasis, they still responded to loading

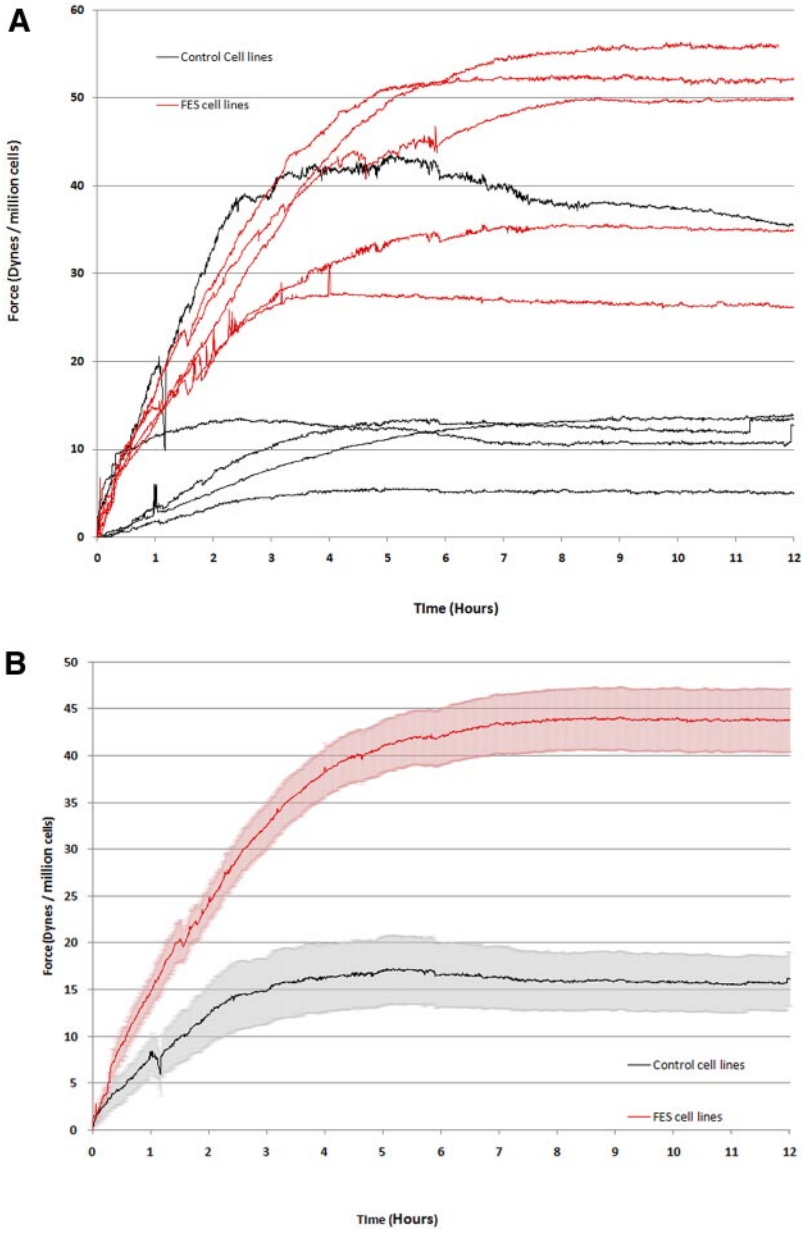

FIGURE 3. Contraction force was altered in FES TFs. On the culture force monitor, collagen gels were seeded with 10^6 cells/mL control or FES tarsal plate fibroblasts, and floated in serum supplemented medium. Cell-free matrices were prepared as the negative control. The force associated with the contraction of the matrix was continuously recorded for 12 hours. (**A**) Force measurements for individual cell lines: each curve represents the mean of three different experiments on the same cell line. (**B**) Average force level for control and FES cells: the arithmetic mean intrinsic force data were calculated from all control and FES samples. The *gray* and *pink* areas surrounding each curve represent the SEM.

and relaxation cycles in a manner similar to the control. To examine this behavior in more detail, we calculated how the rate of change of force varies with the magnitude of force across the gel (Fig. 4B). The best-fit lines broadly define the relationship between external force and the response of the matrix cells, as expressed by the rate of change of force. Overall, our analysis showed that the greater the force change from the baseline level, the greater the rate of change of response from the cells, as expected from a standard tensional homeostasis mechanism. Figure 4B also illustrates that the response trend of FES cell lines is very similar to that of control cell lines, but shifted to the right and centered around a new 0 point moving from 16.2 to 49.4 dynes. This phenomenon is consistent with a change in the mechanostat set point of TFs in FES. In addition, the analysis allows for the estimation of the sensitivity of the cells to mechanical stress. Sensitivity (S) can be expressed as the incremental response (r) per unit intensity of the stimulus (I)—that is, $S = dr/dI$.[27] In other words, sensitivity can be interpreted as the gradient of the best fit lines of representing the FES and control TF responses in the contractility graph illustrated in Figure 4B. The gradients of the best fit lines for FES and control cell lines, representing the sensitivity of the response, were −0.0052 for FES cell lines and −0.0075 for control cell lines, demonstrating a slightly diminished sensitivity for FES cells. Overall, this demonstrates that there is both a reduction in sensitivity of FES TFs when compared with controls and a significant change in the 0 point from 16.2 to 49.2 dynes/million cells.

The responses of control experiments in which unseeded gel matrices are shown, showing that the gels alone also demonstrate similar responses, but at a much lower magnitude and with similar gradient for gels with low levels of force (unseeded control gel for the control) and gels with higher levels of force (unseeded control gel for FES cells). These responses are likely to be the result of a hysteresis phenomenon arising from the complex mechanical behavior of these gels. These control experiments show that the cellular responses, rather than the gel properties, dominate the response phase of the fibroblast-populated gel.

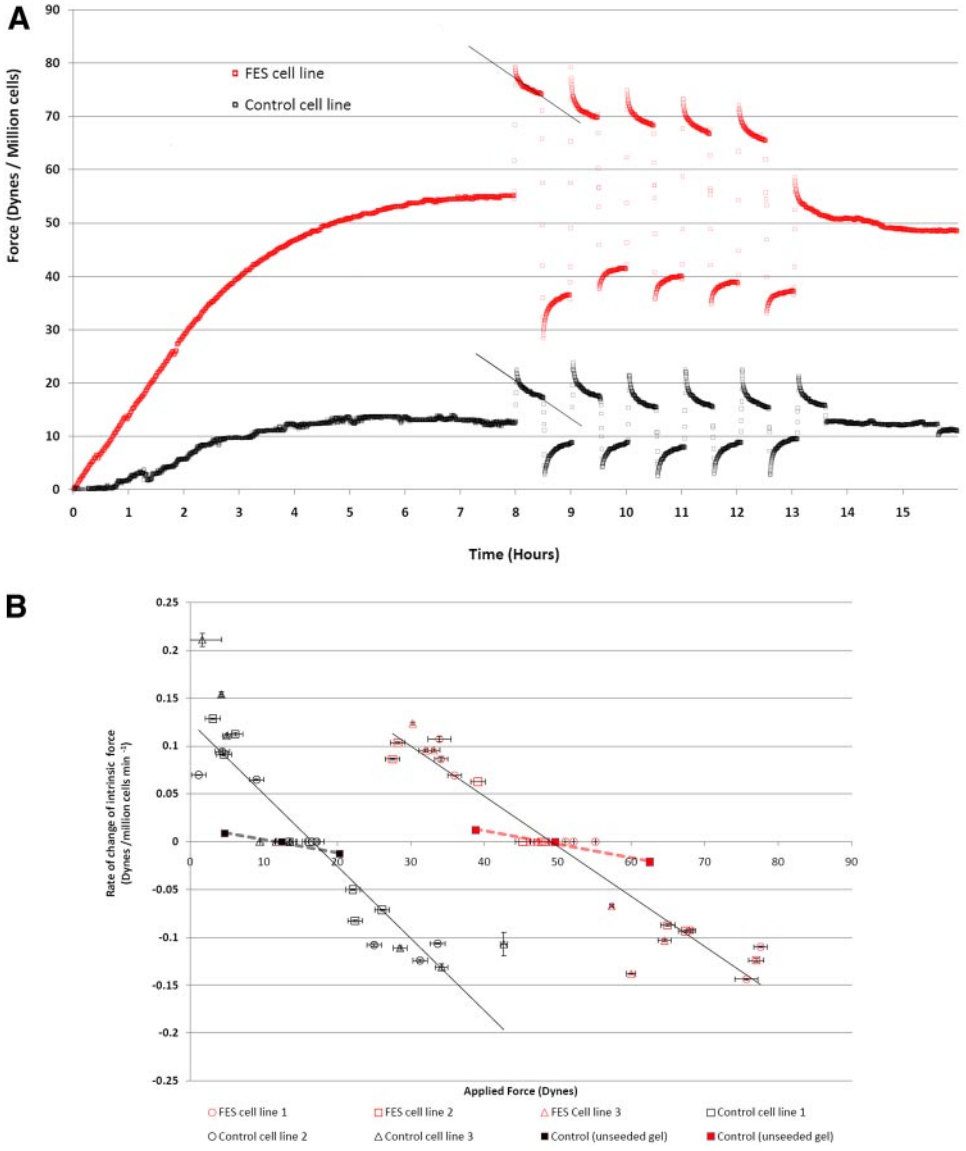

FIGURE 4. Tarsal plate fibroblasts' response to mechanical stress and mechanostat point adjustment. (**A**) Control and FES cell lines were suspended in a collagen matrix and allowed to contract freely while the endogenous force generated by the cells was recorded. At 8 hours, once the plateau phase became established, an external loading force was applied across the gel and maintained for 30 minutes. The subsequent relaxation of the cells was then observed. After 30 minutes, the gel was rapidly unloaded to a state of tension below the plateau. A rapid contractile effect was then observed whereby the endogenous tension was increased across the gel. This cycle was then repeated five times. The graph shows one representative experiment for control and FES cells and illustrates the measurement of a best-fit line through the response curve of the cells, allowing for a gradient to be measured that represents the average rate of change of force generated by the resident fibroblasts over the 30-minute experimental period. Externally applied contraction and relaxation induced an opposing response from the resident cells as they attempted to return to a preferred level of endogenous tension at the plateau level (i.e., tensional homeostasis). (**B**) Mechanostat adjustment in FES cells. The rate of change of force (gradient response, as in **A**) was plotted against the external tension across the gel for each experiment. Contractile forces are represented as positive values and relaxation changes are represented as negative values. The value at tensional homeostasis was also included, with a corresponding *y*-axis value of 0, as there is no change in cell-generated force at the plateau level. In each experiment, cell lines were subjected to five cyclic changes in tension above and below the plateau. For each experiment, the mean force of deflection across the gel was plotted against the mean gradient response. Experiments were performed in triplicate for three FES and three control cell lines. As each data point was generated from five contraction and relaxation episodes in each experiment; horizontal error bars, SEM for tension force across the gel; vertical error bars, SEM of rate of gradient response. Each cell line is plotted three times to represent the triplicate experiments. Best-fit lines are included that demonstrate a maintained tensional homeostasis response that is shifted to the right in FES. Control experiments using acellular gels are included.

Candidate Genes Identified in Gene Expression Microarray Analysis

To investigate what molecular mechanisms could underlie the increased contractile behavior and change in mechanostat level in FES TFs, we first looked for potential changes in the organization of the cells' cytoskeleton, as a high contractile behavior has often been linked in the literature with changes in the filamentous actin organization and more particularly an increase in α-smooth muscle actin (αSMA) expression and incorporation in stress fibers, characteristic of the myofibroblast phenotype.[28] However, no obvious differences in F-actin cytoskeletal organization in FES tarsal cells compared with the control were identified, and no difference in a-SMA expression or incorporation into stress fibers in cells in 2-D monolayers or within the collagen gels was observed (data not shown). In addition, the number of αSMA-positive cells in FES and control samples was not found to be different (5.9% αSMA$^+$, SD 1.3 in FES gels and 5.8% αSMA$^+$, SD 1.8 in control gels, $P = 0.7$ Student's *t*-test).

Three control and three corresponding FES TF cell lines were selected for gene expression microarrays analysis. Only 20 genes with a significant difference in expression between FES and control TFs (Table 2) were identified. Of these genes, nine were regulatory genes: five small nucleolar RNAs (snoRNAs); *HIST1H2BK*, a histone cluster gene; and several cell cycle regulation genes, such as Cyclin D1 and Cyclin D2 and growth arrest specific-6 (*GAS-6*).

Of the remaining 10 genes, the 6 most appropriate candidate genes for differences in the contractility were selected. These were vascular cell adhesion molecule-1 (*VCAM-1*), implicated in the response of endothelial cells subjected to cyclic stress[29] and also in the regulation of sarcoma (Src) protein which is involved in integrin receptor transduction; *PPP1R3C*, the protein phosphatase 1 (PP1) subunit protein targeting to

TABLE 2. Differences in mRNA Expression between FES and Control TFs

Gene Symbol	Gene Description	*P*	Change Ratio (Absolute)	Regulation in FES TF Cell Lines	GenBank* ID
XRRA1	X-ray radiation resistance associated 1	0.001	1.8	Down	BC037294
CCND1	Cyclin D1	0.007	1.5	Up	BC023620
LL22NC03-75B3.6	KIAA1644 protein	0.007	1.6	Up	BC104183
PPP1R3C	Protein phosphatase 1, regulatory (inhibitor) subunit 3C	0.008	1.7	Up	BX537399
GAS6	Growth arrest-specific 6	0.009	1.6	Up	AK126533
SNORD3A	Small nucleolar RNA, C/D box 3A	0.01	1.6	Up	
SNORD3A	Small nucleolar RNA, C/D box 3A	0.01	1.6	Up	
SNORD3A	Small nucleolar RNA, C/D box 3A	0.01	1.6	Up	
SNORD3A	Small nucleolar RNA, C/D box 3A	0.01	1.6	Up	
SNORD3A	Small nucleolar RNA, C/D box 3A	0.01	1.6	Up	
VCAM1	Vascular cell adhesion molecule 1	0.014	2.5	Up	BC017276
CCBE1	Collagen and calcium binding EGF domains 1	0.024	1.6	Up	AB075863
SLC16A4	Solute carrier family 16, member 4 (monocarboxylic acid transporter 5)	0.026	1.5	Up	U59185
HIST1HBK	Histone cluster 1, H2bk	0.026	1.8	Up	BC108737
PRSS12	Protease, serine, 12 (neurotrypsin, motopsin)	0.027	1.6	Up	BC007761
VCAN	Versican	0.038	2.0	Down	U16306
TOX	Thymocyte selection-associated high mobility group box	0.040	1.8	Up	AB018351
DPP4	Dipeptidyl-peptidase 4 (CD26, adenosine deaminase complexing protein 2)	0.041	1.8	Down	BC065265
EFEMP1	EGF-containing fibulin-like extracellular matrix protein 1	0.044	1.7	Down	BC098561
CCND2	Cyclin D2	0.046	2.2	Down	D13639

* Available at http://www.ncbi.nlm.nih.gov/Genbank; provided in the public domain by the National Center for Biotechnology Information, Bethesda, MD.

glycogen (PTG) which acts as an inhibitor of protein phosphatase 1 and has a binding site to the cytoplasmic tail of the integrin receptor; collagen and calcium-binding EGF domains 1 (*CCBE1*), a little-understood protein that may be involved in cell motility[30] and has homology with elements of the fibrillin (FIB)-1 protein; versican, a prominent tarsal plate ECM glycosaminoglycan; EGF-containing fibulin-like extracellular matrix protein-1 (*EFEMP-1*), also known as fibulin-3, implicated in the pathogenesis of age related macular degeneration[31] and also known to be associated with abnormalities in the elastic fiber layer of Bruch's membrane[32]; and neurotrypsin (*PRSS-12*), a serine protease involved in tissue remodeling.[33] These genes were selected for further semiquantitative analysis by RT-PCR. Normalized intensity readings for bands in each cell line were compared as control and FES groups (Fig. 5A) and the resulting *P*-values are summarized in Table 3. Only *VCAM-1* and *PPP1R3C* expression were found to be significantly different between the test and control groups (Fig 5B).

DISCUSSION

Cells in the body are constantly exposed to various mechanical stresses as a result of a moving environment and rely on internal mechanisms to maintain tensional homeostasis.[2] Tensional homeostasis has recently been shown to regulate multiple cell features such as cell shape and motility as well as proliferation and differentiation.[34–36] When the balance between the external (matrix) tension and internal (cytoskeletal) tension is perturbed, cells fail to maintain homeostasis, and pathologic outcomes such as scarring, fibrosis, vascular disease, or cartilage damage occur.[34] Several studies suggest that although the level of tensional homeostasis is normally a constant of a given cell type,[7] cells can alter their mechanosensitivity through an adaptive response to chronic changes in their environment.[2,8,10] As a disease where there is a clear alteration in the mechanical properties of the affected tissue, with a well-described associated exposure of the tissue to chronic mechanical stress, FES represents a good paradigm to begin unraveling the mechanisms regulating tensional homeostasis in the body.

We have shown in the current study that TFs in FES present a strikingly different phenotype than the corresponding control cells in their mechanosensing and contractile properties, with a higher mechanostat level and contractile ability and

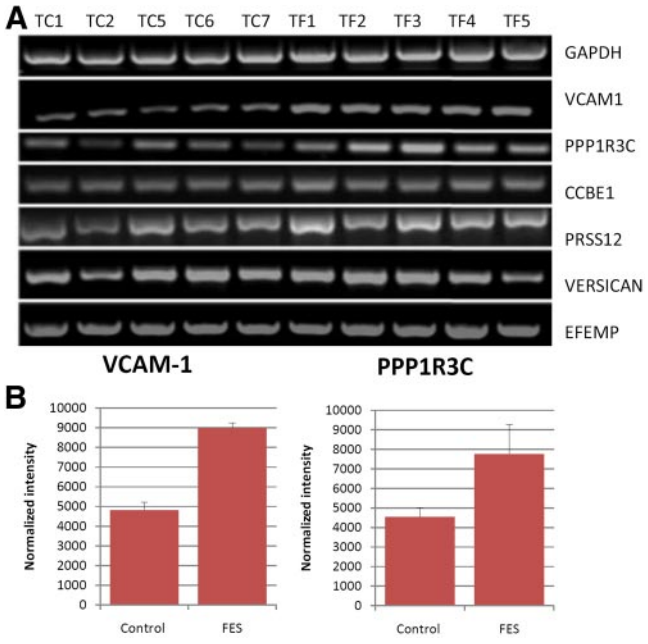

FIGURE 5. FES TFs show altered levels of VCAM-1 and PPP1RC3 mRNA expression. (**A**) RT-PCR analysis: five control and five FES (F) fibroblasts cell lines were analyzed for mRNA expression of seven different genes (*right*). (**B**) Quantitation analysis of (**A**) for the two genes, for which significant differences in expression were measured between the control and FES cells. Data are the mean ± SEM. Corresponding statistical analysis is presented in Table 3.

TABLE 3. Significance of Differences Between Test and Control Groups

Gene Symbol	*P**	Regulation in FES TF Cell Lines
VCAM-1	0.008	Up
PPP1R3C	0.032	Up
CCBE1	0.421	Up
PRSS12	0.095	Up
VCAN	0.691	Down
EFEMP1	0.095	Down

* Mann-Whitney U test.

lower sensitivity to mechanical stretch. The observation that there is no difference in contractility between FES and control tissues for orbicularis or conjunctival fibroblasts, directly adjacent to the tarsal plate, is very likely to be due to the effect of stress shielding of the upper eyelid by the tarsal plate. Stress shielding refers to a phenomenon in load-bearing multimaterial composites, such that the stiffer component of the composite endures the greater part of the load. The tarsal plate is considerably stiffer than the other eyelid components, and it is therefore to be expected that TFs are exposed to the greater load than either orbicularis or conjunctival fibroblasts. Of interest, the fact that differences in the cells' contractile phenotype could be demonstrated even when FES TFs had been in culture at 3 to 4 passage cycles confirms that, as previously suggested,[2,22] the level of force at homeostasis is an intrinsic property of the cells.

The demonstrated increase in intrinsic cellular force generation of FES TFs compared with the control appears paradoxical, as tarsal plate tissue in FES becomes both *hyperelastic* and exposed to prolonged periods of high mechanical loading at night. The tensional homeostasis response predicts that cells reduce their contractility in high-stress environments to maintain a homeostatic tension across the cell cytoskeleton. We hypothesized that this paradoxical response may be due to a change in the mechanostat set point of these cells. We found that FES TFs were able to retain their homeostatic responses, albeit around a different baseline. The homeostatic responses (either of contraction or relaxation) seen in both control and FES TFs were broadly similar for a given magnitude of deflection from the baseline tension.

FES eyelids are commonly stretched for long periods during sleep, and it is likely that this stimulus reprograms the cells to reset their mechanostat set point to a higher level of background tension. This reset would allow the cells to maintain a dynamic range of sensitivity and response at much higher background levels of tension than a normal cell could endure. This effect could correlate with increased intrinsic levels of force and would explain why their baseline contractility is increased relative to the control. Adaptive responses such as this are commonly seen in biological sensory systems, where, for example, in turtle cochlear hair cells, the application of a steady deflection of the hair bundle shifts the operating point, or 0 point, of the transducer,[37] and in photoreceptors, a dramatic change in sensitivity is observed of up to 10,000-fold, depending on the changes in light intensity.[38] Without such adaptive mechanisms, the sensory mechanism would be limited to a relatively small dynamic range. There are different forms of adaptation that allow cells to operate in different dynamic ranges. These include changes in sensitivity, gain, or the operating point of the sensory unit. We have shown that in addition to a change in mechanostat level, tarsal cells in FES present a reduced sensitivity to the mechanical stress (FES sensitivity reduced from −0.0075 to −0.0052 dynes per million cells/min), which again is consistent with an adaptive response.

Tensional homeostasis is well understood as a physiological property of cells but is poorly characterized and investigated in the context of pathologic processes. Only one other study has been identified in which cell contractile homeostatic responses to changes in background tension were investigated. Cultured tendon fibroblasts in Dupuytren's contracture demonstrate increased baseline contractility responses, as in our study, but also a loss of homeostatic response to mechanical stress compared to with that of the control.[39] It is thought that the loss of homeostatic response may be part of the intrinsic fibroblast disease that underlies Dupuytren's contracture. In contrast, the maintained homeostatic response seen in FES TFs would support the conclusion that the increased contractility is an adaptive physiological response rather than a result of fibroblast disease.

The concept of change in mechanostat set point has also been established. Using MMP 13 inhibition as a surrogate endpoint for evaluating cellular response to mechanical loading, it has been demonstrated that tendon cells in vitro can alter their mechanostat set point after 48 hours stress deprivation.[9] The change in mechanostat set point that we observed in this study was observed in cultured FES TFs and was maintained after several passage cycles. This persisting altered response indicates that once the 0-point of these cells has been reprogrammed, their new set point will persist, even in vitro. The mechanisms underlying this change are poorly understood. It has been speculated that disruption of the pericellular ECM may modify normal mechanotransduction mechanisms,[9] and indeed we have additional evidence suggesting that the extracellular matrix is altered both structurally and biochemically in FES (Ezra et al. manuscript in preparation).

The possible mechanisms underlying the changes in contractile behavior in FES were further explored. No co-localization of F-actin and α-SMA was observed, excluding the possibility that myofibroblast differentiation may be responsible. We hypothesized that such significant changes in contractility were likely to manifest a correspondingly significant change in the molecular mechanisms and regulation of either the sensory mechanotransduction arm or effector contractility arm of the cell contractile response. These molecular mechanisms were investigated using a genome level expression microarray platform.

The most striking feature of the expression microarray analysis was the small number of genes identified with significant differences in expression. After selection from the microarray experiment of the most likely candidate genes to be involved, only two were found to be significant: *PPP1R3C* and *VCAM-1*. *PPP1R3C*, or protein phosphatase 1 inhibitory molecule (subunit 3) is an inhibitory subunit of protein phosphatase 1 (PP1). PP1 is a major serine/threonine phosphatase that regulates a very diverse range of cellular functions. The PP1 effector unit is the catalytic unit, or PP1c and this is known to form complexes with approximately 50 regulatory subunits.[40] One of these regulatory subunits is PPP1R3C, also known as R5 or protein targeting to glycogen (PTG).[41] It is ubiquitously distributed, but is more abundant in the liver and in skeletal muscle, and it is thought to regulate PP1c and glycogen synthase-mediated glycogen metabolism.[42,43] PPP1R3C remains poorly characterized and while a role in glucose metabolism has been described, other regulatory functions have not been excluded. Of interest, PPP1R3C knockdown in 3T3L1 cells does not alter PP1 expression but increases the level of PP1 that is bound to other regulatory subunits.[44] Assuming the reverse is true, the increase in PPP1R3C expression seen in FES TFs could decrease the accessibility of PP1 to other subunits, leading to a possible increase in phosphorylation levels of the

corresponding target proteins. As several other regulatory subunits of PP1 are targeting the cytoskeleton,[35–37] and particularly myosin,[19] this could explain the increased levels of cell contractility that we observed.

The other highly expressed gene in FES TFs is *VCAM-1*. VCAM-1 is a cell adhesion molecule, and its classic role lies in the recruitment of inflammatory cells through leukocyte-endothelium adhesion in inflammation. Fibroblasts have been shown to express VCAM-1 but this is usually in the context of inflammatory cell recruitment and retention. However, VCAM-1 can also undergo proteolytic cleavage and exist as a soluble molecule, which has recently been shown to change cell morphology by activation of extracellular signal-regulated kinase (ERK) and Src.[45] Both ERK and Src are important regulators of integrin mechanotransduction in fibroblasts and can affect the transduction mechanism at multiple levels.[40,46]

Changes in both VCAM-1 expression and PP1 modulation are consistent with current etiologic theories of stress-induced hyperelasticity and ischemia–reperfusion injury.[47] VCAM-1 expression has been shown to be altered in cells subjected to pathologic mechanical stress[48] and also in the context of tissue ischemia.[49] Protein phosphatase 1 regulation is similarly recognized in the response to both ischemia reperfusion injury[50] and cyclic mechanical stress.[51]

Conclusions

In conclusion, TFs in FES demonstrate a maintained tensional homeostasis response operating at an altered mechanostat set point and lower sensitivity to mechanical stress. We propose that this change in the 0 point is an adaptation that allows tensional homeostasis to be maintained at the high levels of tissue stress experienced in FES. Gene expression studies point to a role for VCAM-1 and PPP1R3C in mediating changes in the dynamic range of mechanosensitivity of TFs.

References

1. Jones D. How do cells respond to the mechanical environment. In: Reglin G, ed. Wolff's Law and connective tissue regulation. *Berlin Walterde Guyter*. 1992:135–145.
2. Brown RA, Prajapati R, McGrouther DA, Yannas IV, Eastwood M. Tensional homeostasis in dermal fibroblasts: mechanical responses to mechanical loading in three-dimensional substrates. *J Cell Physiol.* 1998;175:323–332.
3. Wang N, Butler JP, Ingber DE. Mechanotransduction across the cell surface and through the cytoskeleton. *Science.* 1993;260:1124–1127.
4. Solon J, Levental I, Sengupta K, Georges PC, Janmey PA. Fibroblast adaptation and stiffness matching to soft elastic substrates. *Biophys J.* 2007;93:4453–4461.
5. Georges PC, Janmey PA. Cell type-specific response to growth on soft materials. *J Appl Physiol.* 2005;98:1547–1553.
6. Mizutani T, Haga H, Kawabata K. Cellular stiffness response to external deformation: tensional homeostasis in a single fibroblast. *Cell Motil Cytoskeleton.* 2004;59:242–248.
7. Frost HM. Bone. "mass" and the "mechanostat": a proposal. *Anat Rec.* 1987;219:1–9.
8. Chicurel ME, Chen CS, Ingber DE. Cellular control lies in the balance of forces. *Curr Opin Cell Biol.* 1998;10:232–239.
9. Arnoczky SP, Lavagnino M, Egerbacher M, Caballero O, Gardner K, Shender MA. Loss of homeostatic strain alters mechanostat "set point" of tendon cells in vitro. *Clin Orthop Relat Res.* 2008;466:1583–1591.
10. Donahue HJ. Gap junctional intercellular communication in bone: a cellular basis for the mechanostat set point. *Calcif Tissue Int.* 1998;62:85–88.
11. Ezra DG, Beaconsfield M, Collin JR. Surgical anatomy of the upper eyelid: old controversies, new concepts. *Expert Rev Ophthalmol.* 2009;4:47–57.
12. Culbertson WW, Ostler HB. The floppy eyelid syndrome. *Am J Ophthalmol.* 1981;92:568–575.
13. Schlotzer-Schrehardt U, Stojkovic M, Hofmann-Rummelt C, Cursiefen C, Kruse FE, Holbach LM. The pathogenesis of floppy eyelid syndrome: involvement of matrix metalloproteinases in elastic fiber degradation. *Ophthalmology.* 2005;112:694–704.
14. Goldberg R, Seiff S, McFarland J, Simons K, Shorr N. Floppy eyelid syndrome and blepharochalasis. *Am J Ophthalmol.* 1986;102:376–381.
15. Culbertson WW, Tseng SC. Corneal disorders in floppy eyelid syndrome. *Cornea.* 1994;13:33–42.
16. Netland PA, Sugrue SP, Albert DM, Shore JW. Histopathologic features of the floppy eyelid syndrome: involvement of tarsal elastin. *Ophthalmology.* 1994;101:174–181.
17. Imbert P, Williamson W, Leger F, Gauthier L, Lagoutte F. Bilateral corneal neovascularization and floppy eyelid syndrome. A case report (in French). *J Fr Ophtalmol.* 1990;13:223–225.
18. Rossiter JD, Ellingham R, Hakin KN, Twomey JM. Corneal melt and perforation secondary to floppy eyelid syndrome in the presence of rheumatoid arthritis. *Br J Ophthalmol.* 2002;86:483.
19. Valenzuela AA, Sullivan TJ. Medial upper eyelid shortening to correct medial eyelid laxity in floppy eyelid syndrome: a new surgical approach. *Ophthal Plast Reconstr Surg.* 2005;21:259–263.
20. Ezra DG, Beaconsfield M, Sira M, et al. Long-term outcomes of surgical approaches to the treatment of floppy eyelid syndrome. *Ophthalmology*. 2010117(4):839–846.
21. Ezra DG, Beaconsfield M, Sira M, Bunce C, Wormald R, Collin R. The Associations of floppy eyelid syndrome: a case control study. *Ophthalmology*. 2010;117(4):831–838.
22. Dahlmann-Noor AH, Martin-Martin B, Eastwood M, Khaw PT, Bailly M. Dynamic protrusive cell behaviour generates force and drives early matrix contraction by fibroblasts. *Exp Cell Res.* 2007;313:4158–4169.
23. Eastwood M, McGrouther DA, Brown RA. A culture force monitor for measurement of contraction forces generated in human dermal fibroblast cultures: evidence for cell-matrix mechanical signalling. *Biochim Biophys Acta.* 1994;1201:186–192.
24. Eastwood M, Porter R, Khan U, McGrouther G, Brown R. Quantitative analysis of collagen gel contractile forces generated by dermal fibroblasts and the relationship to cell morphology. *J Cell Physiol.* 1996;166:33–42.
25. Bailly M, Macaluso F, Cammer M, Chan A, Segall JE, Condeelis JS. Relationship between Arp2/3 complex and the barbed ends of actin filaments at the leading edge of carcinoma cells after epidermal growth factor stimulation. *J Cell Biol.* 1999;145:331–345.
26. Irizarry RA, Hobbs B, Collin F, et al. Exploration, normalization, and summaries of high density oligonucleotide array probe level data. *Biostatistics.* 2003;4:249–264.
27. Torre V, Ashmore JF, Lamb TD, Menini A. Transduction and adaptation in sensory receptor cells. *J Neurosci.* 1995;15:7757–7768.
28. Tomasek JJ, Gabbiani G, Hinz B, Chaponnier C, Brown RA. Myofibroblasts and mechano-regulation of connective tissue remodelling. *Nat Rev Mol Cell Biol.* 2002;3:349–363.
29. Barron V, Brougham C, Coghlan K, et al. The effect of physiological cyclic stretch on the cell morphology, cell orientation and protein expression of endothelial cells. *J Mater Sci Mater Med.* 2007;18:1973–1981.
30. Yamamoto F, Yamamoto M. Scanning copy number and gene expression on the 18q21-qter chromosomal region by the systematic multiplex PCR and reverse transcription-PCR methods. *Electrophoresis.* 2007;28:1882–1895.
31. Marmorstein LY, McLaughlin PJ, Peachey NS, Sasaki T, Marmorstein AD. Formation and progression of sub-retinal pigment epithelium deposits in Efemp1 mutation knock-in mice: a model for the early pathogenic course of macular degeneration. *Hum Mol Genet.* 2007;16:2423–2432.
32. Chong NH, Keonin J, Luthert PJ, et al. Decreased thickness and integrity of the macular elastic layer of Bruch's membrane correspond to the distribution of lesions associated with age-related macular degeneration. *Am J Pathol.* 2005;166:241–251.

33. Gschwend TP, Krueger SR, Kozlov SV, Wolfer DP, Sonderegger P. Neurotrypsin, a novel multidomain serine protease expressed in the nervous system. *Mol Cell Neurosci.* 1997;9:207–219.
34. Ingber DE. Cellular mechanotransduction: putting all the pieces together again. *FASEB J.* 2006;20:811–827.
35. McBeath R, Pirone DM, Nelson CM, Bhadriraju K, Chen CS. Cell shape, cytoskeletal tension, and RhoA regulate stem cell lineage commitment. *Dev Cell.* 2004;6:483–495.
36. Vogel V, Sheetz M. Local force and geometry sensing regulate cell functions. *Nat Rev Mol Cell Biol.* 2006;7:265–275.
37. Crawford AC, Evans MG, Fettiplace R. Activation and adaptation of transducer currents in turtle hair cells. *J Physiol.* 1989;419:405–434.
38. Burkhardt DA. Light adaptation and photopigment bleaching in cone photoreceptors in situ in the retina of the turtle. *J Neurosci.* 1994;14:1091–1105.
39. Bisson MA, Mudera V, McGrouther DA, Grobbelaar AO. The contractile properties and responses to tensional loading of Dupuytren's disease-derived fibroblasts are altered: a cause of the contracture? *Plast Reconstr Surg.* 2004;113:611–621, discussion 622–614.
40. Cohen PT. Protein phosphatase 1: targeted in many directions. *J Cell Sci.* 2002;115:241–256.
41. Doherty MJ, Young PR, Cohen PT. Amino acid sequence of a novel protein phosphatase 1 binding protein (R5) which is related to the liver- and muscle-specific glycogen binding subunits of protein phosphatase 1. *FEBS Lett.* 1996;399:339–343.
42. Printen JA, Brady MJ, Saltiel AR. PTG, a protein phosphatase 1-binding protein with a role in glycogen metabolism. *Science.* 1997;275:1475–1478.
43. Fong NM, Jensen TC, Shah AS, Parekh NN, Saltiel AR, Brady MJ. Identification of binding sites on protein targeting to glycogen for enzymes of glycogen metabolism. *J Biol Chem.* 2000;275:35034–35039.
44. Greenberg CC, Danos AM, Brady MJ. Central role for protein targeting to glycogen in the maintenance of cellular glycogen stores in 3T3–L1 adipocytes. *Mol Cell Biol.* 2006;26:334–342.
45. Ueki S, Kihara J, Kato H, et al. Soluble vascular cell adhesion molecule-1 induces human eosinophil migration. *Allergy.* 2009;64:718–724.
46. Katsumi A, Orr AW, Tzima E, Schwartz MA. Integrins in mechanotransduction. *J Biol Chem.* 2004;279:12001–12004.
47. Ezra DG, Beaconsfield M, Collin R. Floppy eyelid syndrome: stretching the limits. *Surv Ophthalmol.* 2010;55:35–46.
48. Smith KE, Metzler SA, Warnock JN. Cyclic strain inhibits acute pro-inflammatory gene expression in aortic valve interstitial cells. *Biomech Model Mechanobiol.* 2010;9:117–125.
49. Blann A, Kumar P, Krupinski J, McCollum C, Beevers DG, Lip GY. Soluble intercellular adhesion molecule-1, E-selectin, vascular cell adhesion molecule-1 and von Willebrand factor in stroke. *Blood Coagul Fibrinolysis.* 1999;10:277–284.
50. Nicolaou P, Rodriguez P, Ren X, et al. Inducible expression of active protein phosphatase-1 inhibitor-1 enhances basal cardiac function and protects against ischemia/reperfusion injury. *Circ Res.* 2009;104:1012–1020.
51. Mills I, Murata K, Packer CS, Sumpio BE. Cyclic strain stimulates dephosphorylation of the 20kDa regulatory myosin light chain in vascular smooth muscle cells. *Biochem Biophys Res Commun.* 1994;205:79–84.